

Structure and magnetic properties of a sulfur–nitrogen radical, methylbenzodithiazolyl†

Gordon D. McManus,^a Jeremy M. Rawson,^{*a} Neil Feeder,^a Fernando Palacio^{*b} and Patricia Oliete^b

^aDepartment of Chemistry, The University of Cambridge, Lensfield Road, Cambridge, UK CB2 1EW. E-mail: jmr31@cam.ac.uk

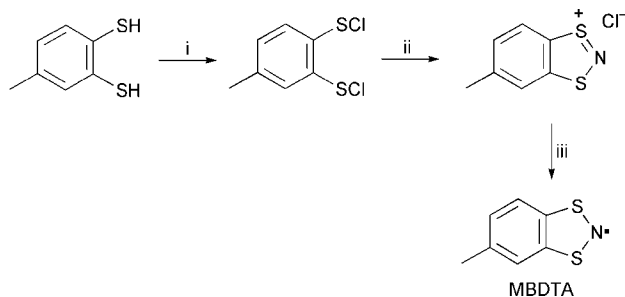
^bInstituto de Ciencia de Materiales de Aragon, CSIC-Universidad de Zaragoza, Zaragoza, Spain E-50009

Received 22nd June 2000, Accepted 12th July 2000
 Published on the Web 4th August 2000

An X-ray crystal structure of the methylbenzodithiazolyl radical MeC₆H₃S₂N, MBDTA, reveals that it forms a regularly spaced π -stack motif in the solid state; variable temperature magnetic studies show that the susceptibility passes through a broad maximum at 140 K indicative of exceptionally strong antiferromagnetic coupling for an organic radical possessing extended magnetic interactions. Its behaviour can be modelled as a two-dimensional Heisenberg square lattice of $S=1/2$ ions with $J=-72$ K.

Wölmershauser first described¹ the syntheses and characterisation of the benzo-fused dithiazolyl radicals BDTA and MBDTA in 1984, and reported that both BDTA and MBDTA showed no tendency to dimerise in the solid state. Whilst solution EPR studies by Passmore² *et al.* on BDTA determined the dimerisation energy to be ~ 0 kJ mol⁻¹, their crystallographic study² showed that BDTA crystallised as a centrosymmetric dimer in the solid state with an S...S separation of 3.175(1) Å. The two unpaired electrons form a multi-centre bonding interaction *via* a $\pi^*-\pi^*$ interaction between singly occupied molecular orbitals (SOMOs), thereby rendering the compound diamagnetic.² Nevertheless, the small dimerisation energy indicates that a fine balance is to be expected between monomeric and dimeric structures. We now report the structure and magnetic properties of MBDTA.

MBDTA was prepared according to the literature method¹ (Scheme 1), although the final reduction step proved problematic and was dependent on reducing agent and solvent. The optimum recovered yield (11% based on 3,4-dimercapto-toluene) used Ag powder in MeCN.‡ Similar problems have been encountered by Oakley *et al.* during the synthesis of the benzobis(dithiazolyl), BBDTA.³

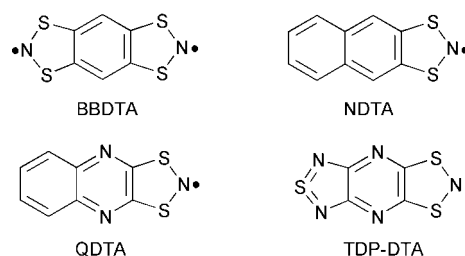


Scheme 1 Reagents and conditions: (i) SO₂Cl₂, reflux CH₂Cl₂; (ii) Me₃SiN₃, CH₂Cl₂, 0 °C; (iii) Ag powder, MeCN.

†A 3D representation of MBDTA as a PDB file is available as supplementary data. For direct electronic access see <http://www.rsc.org/suppdata/jm/b0/b004992l/>

Crystals of MBDTA suitable for single crystal X-ray studies were formed as black rhombs by vacuum sublimation (10⁻² Torr, 50–55 °C), just below the decomposition temperature (60 °C). The asymmetric unit of MBDTA contains a single molecule of unexceptional geometry⁴ (Fig. 1) with the fused ring essentially planar (maximum deviation is for the heterocyclic N which lies 0.035 Å above the mean plane). Molecules of MBDTA form a herringbone array with π -stacking along the crystallographic *c*-axis in a similar manner to NDTA⁵ rather than the slipped π -stacks observed for BBDTA, QDTA and TDP-DTA.⁶

The distance between equivalent atoms in neighbouring rings in the stack coincides with the length of the *c*-axis [5.851(3) Å], but the molecular plane is inclined at 60.7° to the *ab* plane and the closest contact (*d*₃ in Fig. 2) along the stacking direction is 3.742 Å. A view of MBDTA in the *ab* plane is shown in Fig. 3. In addition to the intra-stack contacts, there are a series of inter-stack S...S contacts in the range 3.708–3.819 Å (Fig. 2). All of these intermolecular S...S contacts fall outside the sum of the minor van der Waals radii⁷ for S (~ 3.2 Å), but within the sum of the major van der Waals radii (~ 4.0 Å). These intermolecular contacts give rise to a two-dimensional sheet of interactions in the crystallographic *bc* plane.



Variable temperature dc magnetic susceptibility studies (1.8–300 K) were carried out on a polycrystalline sample of MBDTA on a SQUID magnetometer in an applied field of 1 T. Additional isothermal magnetisation measurements were made at 1.8 and 3 K. Diamagnetic corrections were made for the sample holder and sample (Pascal's constants). A plot of

‡Analytical data for MBDTA: Calcd for C₇H₆NS₂: C, 50.0%; H 3.6%; N, 8.3%; Found C, 49.2%; H, 3.6%; N, 8.3%; EPR (CH₂Cl₂, 298 K), $g=2.003$, $a_N=11.4$ G.

§Crystal data for MBDTA: C₇H₆NS₂, $M=168.25$, orthorhombic, space group *Pbca*, $a=16.778(6)$, $b=14.757(4)$, $c=5.851(3)$ Å, $Z=8$, $T=180(2)$ K, $\mu(\text{Mo-K}\alpha)=0.645$ mm⁻¹. Of 2065 reflections measured, 1268 were unique ($R_{\text{int}}=0.0479$) and were used in all calculations. The final $wR_2=0.1315$ (all data), $R_1 [F > 2\sigma(F)]=0.0523$. CCDC 1145/235. See <http://www.rsc.org/suppdata/jm/b0/b004992l/> for crystallographic files in .cif format.

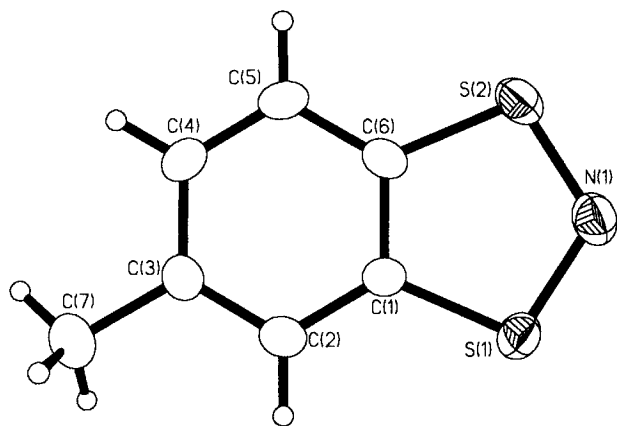


Fig. 1 Selected intramolecular bond lengths (Å) and angles (°) for MBDTA are: S(1)–N(1) 1.653(3), S(1)–C(1) 1.743(4), S(2)–N(1) 1.656(4), S(2)–C(6) 1.740(4), C(1)–C(6) 1.394(5), N(1)–S(1)–C(1) 99.7(2), N(1)–S(2)–C(6) 99.9(2), S(1)–N(1)–S(2) 113.8(6), C(6)–C(1)–S(1) 113.43(3), C(1)–C(6)–S(2) 113.2(2).

the molar susceptibility vs. temperature (Fig. 4) exhibits a broad maximum at 140 K. The absence of any field dependent magnetisation below 140 K indicates that the maximum in χ is associated with the onset of low dimensional antiferromagnetic order. This exceptionally high temperature for χ_{\max} is indicative of very strong antiferromagnetic exchange interactions between spins and this is reflected in the room temperature effective magnetic moment [*ca.* $1.3\mu_B$ at 300 K] which is considerably less than that expected for an $S=1/2$ paramagnet [*ca.* $1.7\mu_B$]. Below *ca.* 25 K the susceptibility curve increases rather sharply most likely due to the contribution from a small mole fraction of non correlated paramagnetic centres in the sample. The paramagnetic origin of such an increase is confirmed by the isothermal magnetisation measurements at 1.8 and 3.0 K which can be fitted to the Brillouin function corresponding to $0.8 \pm 0.1\%$ of $S=1/2$ paramagnetic centers plus a term which depends linearly on the magnetic field. This term combines the (negative) diamagnetic contribu-

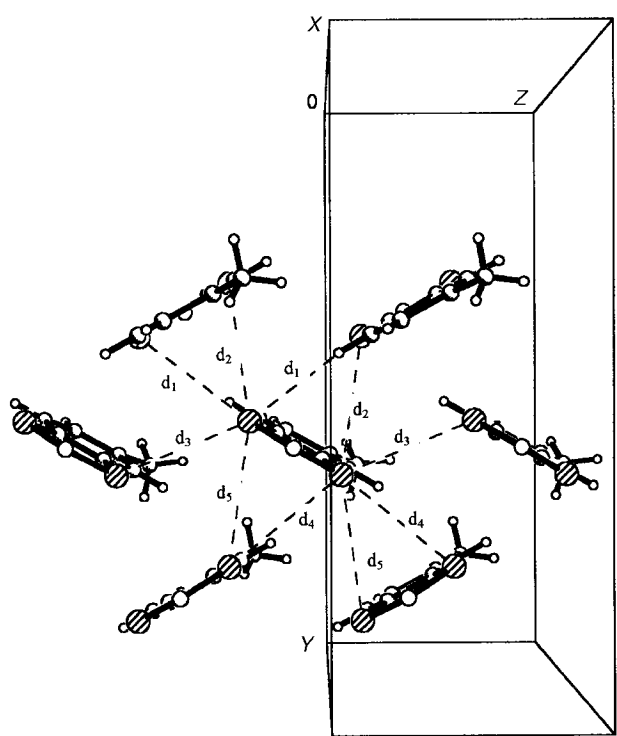


Fig. 2 Molecular packing diagram of MBDTA viewed perpendicular to the crystallographic *a* axis. Selected intermolecular S...S contacts are: $d_1=3.708$, $d_2=3.719$, $d_3=3.742$, $d_4=3.768$, $d_5=3.819$ Å.

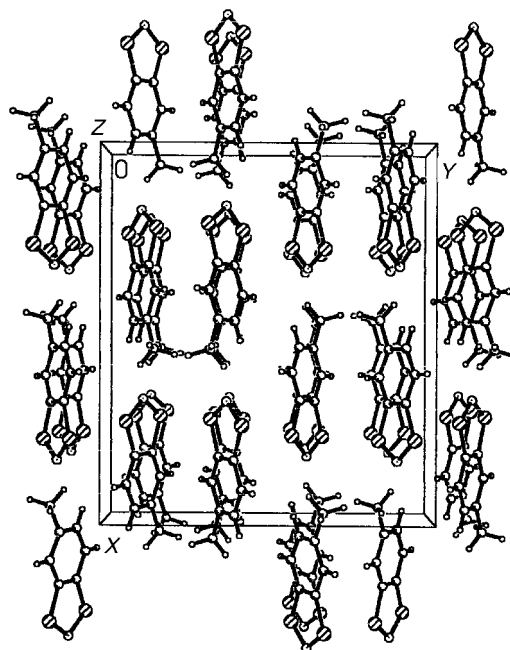


Fig. 3 Molecular packing of MBDTA viewed in the *ab* plane, illustrating the strongly slipped π -stack along the crystallographic *c*-axis and the large separation of dithiazolyl-rich planes along the crystallographic *a*-axis.

tion and the (positive) contribution from the antiferromagnetic correlations.

The low dimensionality of the magnetic structure is consistent with the two-dimensional nature of the dithiazolyl interactions in the crystal structure and the compound was analysed as a two dimensional Heisenberg system, using high temperature series expansions for the square planar Heisenberg model.⁸ A good agreement between experimental and calculated data was observed with an exchange term, $J=-72$ K. The adequacy of the fit was reflected in the excellent comparison between theoretical and experimental values of both the position, $\tau_m=k_B T_{\max}/|J|S(S+1)$, and height, $\chi_m=\chi_{\max}|J|/N g^2 \mu_B^2$, of the maximum of the susceptibility in reduced units (Fig. 5). In the square planar Heisenberg model the theoretical values for these constants are, respectively, 2.495 and 0.0469 for $S=1/2$.⁸ These values are in good agreement with the calculated values $\tau_m=2.578$ and $\chi_m=0.0466$, using $|J|/k_B=72$ K and $g=2$.

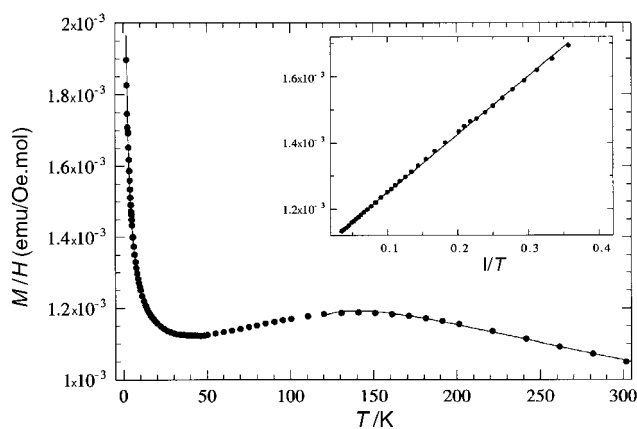


Fig. 4 Variation of molar susceptibility of MBDTA (●) as a function of temperature. The solid line in the high temperature region represents the best fit to the two-dimensional square-planar Heisenberg model, with $J=-72(\pm 1)$ K; in the low temperature region the solid line represents the best fit to the presence of non-correlated paramagnetic centres in the 2D system (see text). The inset shows the Curie behaviour of the paramagnetic centres.

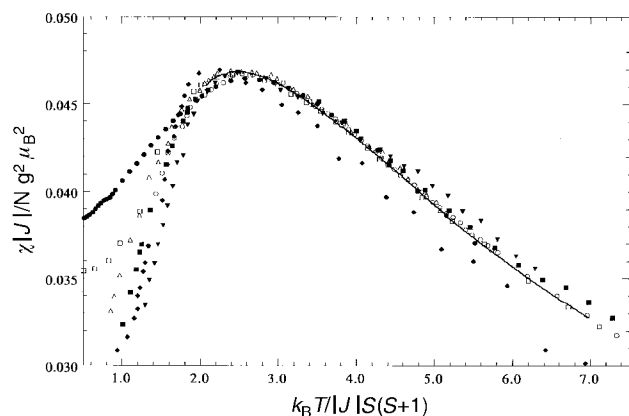


Fig. 5 Experimental temperature dependence of the susceptibility, in reduced units, of MBDTA (●) compared to representative examples of the $S=1/2$ square planar Heisenberg antiferromagnetic model; $[\text{Cu}(\text{C}_5\text{H}_5\text{NO})_6(\text{BF}_4)_2]$ (△), $\text{CuF}_2 \cdot 2\text{H}_2\text{O}$ (□), $(2\text{-NH}_2\text{-5-Cl-C}_5\text{H}_3\text{N})_2\text{CuBr}_4$ (○), $(2\text{-NH}_2\text{-5-Me-C}_5\text{H}_3\text{N})_2\text{CuBr}_4$ (◊), $[\text{Cu}(\text{pz})_2(\text{NO}_3)]\text{PF}_6$ (◆), $[\text{Cu}(\text{pz})_2][\text{ClO}_4]_2$ (▼). Data are scaled to the high temperature series prediction (solid line).

The two-dimensional magnetic behaviour of MBDTA compares very well with other representative examples of the $S=1/2$ square planar Heisenberg model. In Fig. 5 the magnetic susceptibility of MBDTA, corrected for diamagnetic and uncorrelated paramagnetic contributions, is represented in reduced units together with that of $\text{Cu}(\text{C}_5\text{H}_5\text{NO})_6(\text{BF}_4)_2$,⁸ $\text{CuF}_2 \cdot 2\text{H}_2\text{O}$,⁸ $(2\text{-NH}_2\text{-5-Cl-C}_5\text{H}_3\text{N})_2\text{CuBr}_4$,^{9,10} $(2\text{-NH}_2\text{-5-Me-C}_5\text{H}_3\text{N})_2\text{CuBr}_4$,^{9,10} $[\text{Cu}(\text{pz})_2(\text{NO}_3)]\text{PF}_6$ ¹⁰ and $\text{Cu}(\text{pz})_2(\text{ClO}_4)_2$ ¹⁰ as taken from the literature. It is now well theoretically established that a 2D $S=1/2$ square lattice Heisenberg antiferromagnet will order at $T=0$ K.¹¹ However, small deviations from this model can trigger magnetic ordering. Thus, magnetic anisotropy would allow a crossover in the spin dimensionality to the 2D Ising model which can undergo magnetic ordering at a finite temperature. Magnetic interactions between layers would cause a crossover in the lattice dimensionality to the 3D Heisenberg model which would also allow magnetic ordering at finite temperature. The consequence of either kind of crossover, or of both, is that eventually all 2D Heisenberg systems show magnetic ordering at temperatures well below that of the susceptibility maximum (T_{max}). Thus, $\text{Cu}(\text{C}_5\text{H}_5\text{NO})_6(\text{BF}_4)_2$ shows the maximum of the susceptibility at $T_{\text{max}}=1.9$ K and it orders at $T_{\text{N}}=0.62$ K¹² with a ratio $T_{\text{N}}/T_{\text{max}}=0.33$. Other examples are $\text{CuF}_2 \cdot 2\text{H}_2\text{O}$ ($T_{\text{max}}=26$ K, $T_{\text{N}}=10.9$ K¹³ and $T_{\text{N}}/T_{\text{max}}=0.42$), $(2\text{-NH}_2\text{-5-Cl-C}_5\text{H}_3\text{N})_2\text{CuBr}_4$ ($T_{\text{max}}=1.06$ K, $T_{\text{N}}=0.74$ K⁹ and $T_{\text{N}}/T_{\text{max}}=0.70$) and $(2\text{-NH}_2\text{-5-Me-C}_5\text{H}_3\text{N})_2\text{CuBr}_4$ ($T_{\text{max}}=0.82$ K, $T_{\text{N}}=0.44$ K⁹ and $T_{\text{N}}/T_{\text{max}}=0.54$). In the case of MBDTA, despite the very large exchange interaction between radicals, long range order does not seem to become apparent down to 1.8 K, the lowest temperature measured during these experiments. The magnetic ordering transition in $\chi(T)$ measurements is normally manifested as a kink in the $\chi(T)$ curve, but the contribution from uncorrelated paramagnetic centres renders its observation difficult in this instance. In addition, $M(H)$ measurements provide no indication of the presence of antiferromagnetic ordering at 1.8 K either. A low

anisotropy antiferromagnet will normally show a transition from the antiferromagnetic to the spin-flop state in the isothermal magnetisation curve.

Whilst the fused nature of the BDTA and MBDTA ring systems provides an opportunity for π -delocalisation of the spin density away from the heterocyclic ring, theoretical calculations have shown² that the majority of the spin density is still localised on the S and N atoms. Consequently the main pathway for magnetic exchange can be considered to be *via* the intermolecular $\text{S}\cdots\text{N}$ and $\text{S}\cdots\text{S}$ interactions already described. This gives rise to a two-dimensional sheet structure in the bc plane; propagation along the crystallographic a direction relies on $\text{N}\cdots\text{H}$ interactions [at 3.7 Å to the H atom attached to C(4)] and the degree of spin delocalisation onto the C_6 ring (Fig. 3). It is, presumably, the weakness of this third interaction which precludes the onset of long range magnetic order. We are presently examining new derivatives in which more extensive π -delocalisation onto the substituents is anticipated, thereby paving the way towards long range magnetic order at high temperature.

Acknowledgements

We would like to thank the Royal Society for an equipment grant (J.M.R.), the EPSRC for a studentship (G.D.M.) and the CICYT (Grant. No. MAT97-0951) for financial support.

References

- 1 G. Wölmshäuser, M. Schnauber and T. Wilhelm, *J. Chem. Soc., Chem. Commun.*, 1984, 573.
- 2 E. G. Awere, N. Burford, C. Mailer, J. Passmore, M. J. Schriver, P. S. White, A. J. Banister, H. Oberhammer and L. H. Sutcliffe, *J. Chem. Soc., Chem. Commun.*, 1987, 66; E. G. Awere, N. Burford, R. C. Haddon, S. Parsons, J. Passmore, J. V. Waszczak and P. S. White, *Inorg. Chem.*, 1990, **29**, 4821.
- 3 T. M. Barclay, A. W. Cordes, R. H. de Laat, J. D. Goddard, R. C. Haddon, D. Y. Jeter, R. C. Mawhinney, R. T. Oakley, T. T. M. Palstra, G. W. Patenaude, R. W. Reed and N. P. C. Westwood, *J. Am. Chem. Soc.*, 1997, **119**, 2633.
- 4 J. M. Rawson and G. D. McManus, *Coord. Chem. Rev.*, 1999, **189**, 135.
- 5 T. M. Barclay, A. W. Cordes, N. George, R. C. Haddon, R. T. Oakley, T. T. M. Palstra, G. W. Patenaude, R. W. Reed, J. F. Richardson and H. Zhang, *Chem. Commun.*, 1997, 873.
- 6 T. M. Barclay, A. W. Cordes, N. A. George, R. C. Haddon, M. E. Itkis, M. S. Mashuta, R. T. Oakley, G. W. Patenaude, R. W. Reed, J. F. Richardson and H. Zhang, *J. Am. Chem. Soc.*, 1998, **120**, 352.
- 7 S. C. Nyburg and C. H. Faerman, *Acta Crystallogr., Sect. B*, 1985, **41**, 274.
- 8 R. Navarro, in *Magnetic Properties of Layered Transition Metal Compounds*, ed. L. J. de Jongh, Kluwer Academic Publishers, 1990, p. 105.
- 9 P. R. Hammar, D. C. Dender, D. H. Reich, A. S. Albrecht and C. P. Landee, *J. Appl. Phys.*, 1997, **81**, 4615.
- 10 M. M. Turnbull, A. S. Albrecht, G. B. Jameson, C. P. Landee, *Mol. Cryst. Liq. Cryst.*, 1999, **335**, 245.
- 11 N. D. Mermin and H. Wagner, *Phys. Rev. Lett.*, 1966, **17**, 1133.
- 12 R. Navarro, H. A. Algra, L. J. de Jongh, R. L. Carlin and C. J. O'Connor, *Physica B*, 1977, **86-88**, 693.
- 13 S. Tazawa, K. Nagata and M. Date, *J. Phys. Soc. Jpn.*, 1973, **20**, 181.